CHARACTERISTICS OF SLUMGULLION LANDSLIDE INFERRED FROM SUBSURFACE EXPLORATION, IN-SITU AND LABORATORY TESTING, AND MONITORING

William H. Schulz[1], Jonathan P. McKenna[2], Giulia Biavati[3] & John D. Kibler[4]

[1] *U. S. Geological Survey (e-mail: wschulz@usgs.gov)*
[2] *U. S. Geological Survey (e-mail: jmckenna@usgs.gov)*
[3] *Università di Bologna, Italy (e-mail: biavati@geomin.unibo.it)*
[4] *U. S. Geological Survey (e-mail: kibler@usgs.gov)*

Abstract: Continuous monitoring for 22 months of piezometer and tensiometer nests and displacement and meteorological sensors in the active part of the Slumgullion landslide, southwest Colorado, identified complex relationships between pore pressure and movement. Piezometers were located 3.4 m from a landslide margin while tensiometers were located 21.3 m from the margin. Landslide displacement was continuous and generally steady, although velocity spiked following spring snowmelt. Pore-water pressures along the margin dropped 2 m. Pore-water pressures measured away from the margin increased abruptly following rainfall and snowmelt events but mean values were steady. Landslide velocity correlated positively with pore-water pressures measured away from the margin. Pore-water pressures along the margin increased gradually following snowmelt. Cyclic pressure change along the margin occurred with abrupt decrease during landslide acceleration and increase during deceleration, probably due to changes in dilation of shearing landslide debris. Repeated cycles of this type occurred and probably involved dilatant strengthening of shearing landslide debris during acceleration resulting in deceleration and subsequent consolidation of landslide debris and pore-water pressure increase that aided generation of a subsequent acceleration-deceleration cycle.

INTRODUCTION

The Slumgullion landslide is a translational debris slide (Cruden and Varnes 1996) located in the San Juan Mountains in Hinsdale County, southwestern Colorado, U.S.A. (Figure 1). Part of the landslide has been continuously active for about 300 years (Varnes and Savage 1996). The active part of the landslide is about 3.9 km long, averages about 300 m wide, and has an estimated volume of 20×10^6 m^3 and average depth of about 14 m (Parise and Guzzi 1992). Because of its continuous activity, the landslide presents an exceptional opportunity to study landslide processes and has been the subject of several such efforts. For example, Fleming *et al.* (1999) concluded that annual displacement of the landslide had been about constant during the preceding 100 years and found that the landslide consists of several independent kinematic units that can have differing velocities. They found that velocity varies seasonally, presumably due to changes in pore-water pressures. Savage and Fleming (1996) measured landslide displacement in near-real time during part of 1993 and also found seasonally varying velocity. Coe *et al.* (2003) performed hourly monitoring of landslide displacement, air and soil temperature, snow depth, rainfall, soil water content, and apparently perched-groundwater pressures and found that the landslide moved fastest during the spring and summer and slowest during the winter. They identified generally direct, positive correlation between pore-water pressure measured at a depth of 2.2 m and landslide velocity, but also identified periods of landslide acceleration in response to snowmelt events in the absence of increased pore-water pressure. They inferred that greater surface-water availability and increased pore-water pressures resulted in greater landslide velocity. Baum and Reid (2000) proposed that low-permeability clay layers formed along basal and marginal shear zones effectively isolates the landslide hydrologically from adjacent areas and aids perennial landslide displacement. The landslide has greater spatial density of springs, sinks, ponds, and surface-water drainages than adjacent areas (Fleming *et al*. 1999) and the locations and activity levels of these features vary with time. Evaluation of deeper groundwater conditions within the landslide and their relations with precipitation, snowmelt, and landslide displacement has been lacking from previous studies. Deeper groundwater conditions have remained unexplored because of difficult access onto the landslide.

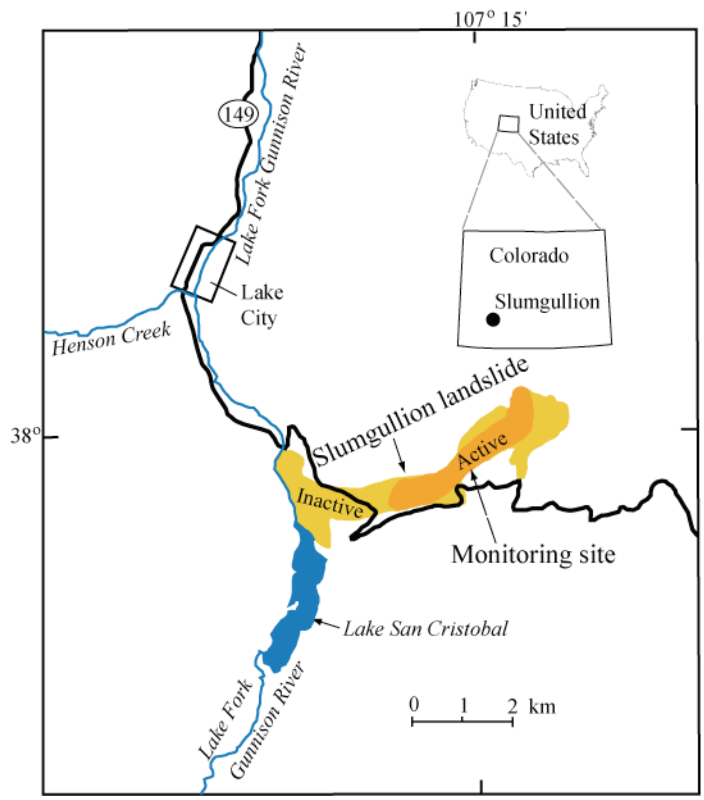

Figure 1. Map showing the location of the Slumgullion landslide. Modified from Coe *et al.* (2003).

To better understand deep groundwater conditions at the landslide, we advanced a borehole during July 2004 to a depth of 9.3 m at a monitoring site (IS-1) described by Coe *et al.* (2003), which is located near the left margin (when viewed in the downhill direction) of the active part of the landslide (Figure 2). The 2.2-m-deep piezometer described by Coe *et al.* (2003) is located about 1 km downslope from where we performed our investigation. We installed equipment to monitor groundwater pressures in saturated and unsaturated landslide debris. This equipment, along with that described by Coe *et al.* (2003), has been monitored on an hourly basis since installation. We performed laboratory and field tests of material properties such as porosity, grain-size distribution, and saturated hydraulic conductivity and installed a subsurface-displacement-measuring device that has been monitored episodically. This paper summarizes the results of this recent work.

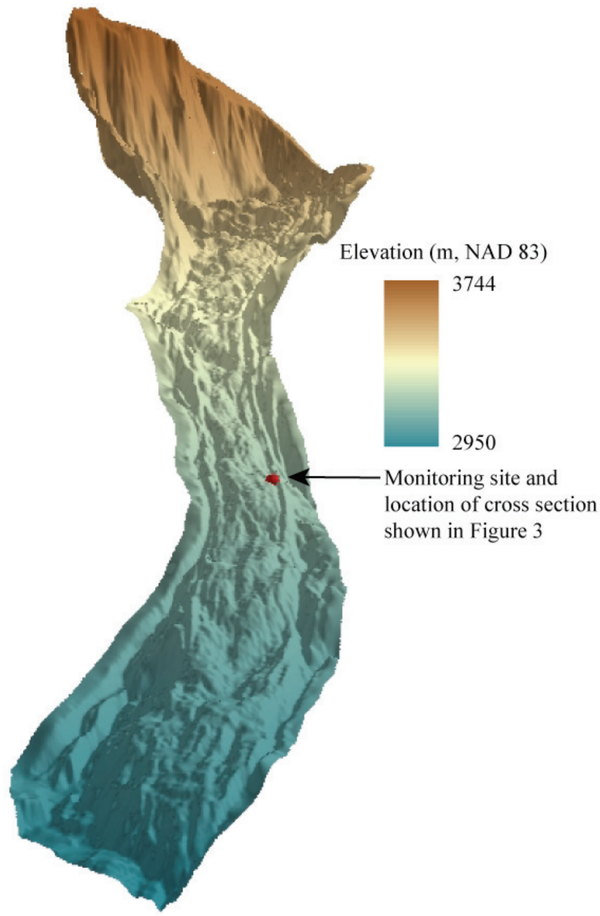

Figure 2. Virtual oblique view of the active part of the Slumgullion landslide developed from digital topographic data (Messerich and Coe 2003). View is from the elevation of the monitoring site, which is represented by the red sphere. The width of the landslide at the monitoring site is about 200 m and the length of the landslide is about 3,900 m.

SETTING

The Slumgullion landslide occurs within Tertiary volcanic rocks including basalt, rhyolite, and andesite, much of which has been highly altered by hydrothermal activity (Lipman 1976; Sharp *et al.* 1983; Diehl and Schuster 1996). The active part of the landslide occurs almost entirely within inactive landslide deposits (Fleming *et al.* 1999, Figure 3). The average inclination of the ground surface along the landslide is 8°. Our monitoring equipment and a monitoring site (IS-1) described by Coe *et al.* (2003) are located at about the middle elevation of the landslide and along its left margin (Figure 2). Nearly all displacement along this margin occurs along the bounding strike-slip fault (Fleming *et al*. 1999). We observed en echelon fractures extending at most about 3 m into the landslide at the monitoring site, measured normal to the strike-slip fault. The monitoring site is about 100 m downslope from the narrowest, fastest part of the landslide (Fleming *et al*. 1999). Average ground-surface inclination is 4° within 100 m upslope and downslope from the monitoring site and 10° beyond this distance for a few hundred meters in both directions.

METHODS

Subsurface exploration and sampling

Topography of the ground surface at the location of our monitoring site is shown on Figure 3, which was developed using measuring tape, pocket transit, and hand level techniques and referenced to the North American Datum 1983 using monuments surveyed with GPS techniques (Coe *et al*. 2003). We constructed our borehole 3.4 m from the strike-slip fault marking the left margin of the landslide using hand-portable, direct-push subsurface exploration equipment manufactured by Geoprobe and driven using an electric breaker hammer powered by a gasoline generator. The borehole was continuously sampled using a 0.6-m-long, 5.1-cm-diameter, cylindrical steel sampler to a depth of 9.3 m where refusal was encountered, presumably on a cobble or boulder. Soil samples were visually classified in accordance with ASTM standards (American Society for Testing and Materials 2002).

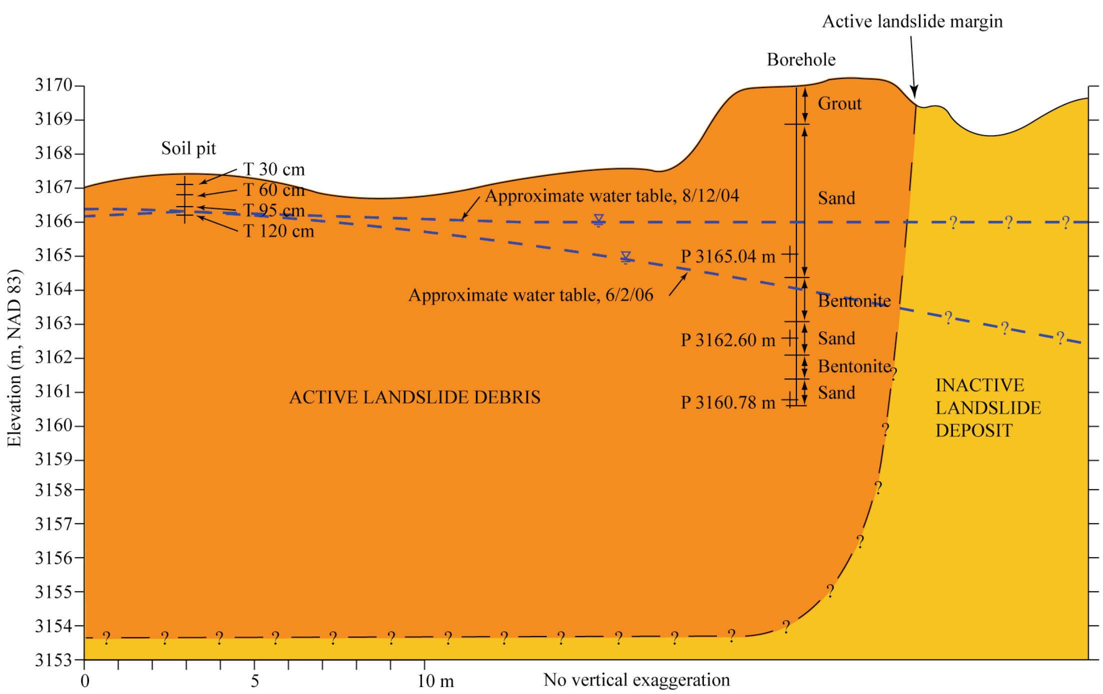

Figure 3. Cross section oriented normal to the landslide margin and extending through the monitoring site. View is oriented parallel to the landslide margin and directed upslope. Tensiometers are indicated by "T" and their depths below the ground surface. Piezometers are indicated by "P" and their elevations. The borehole was backfilled with grout, sand, and bentonite as shown.

We hand excavated one soil pit within the landslide to a depth of 1.4 m. The pit was located 21.3 m from the left margin of the landslide (Figure 3). Relatively undisturbed soil samples were obtained from depths of 30, 60, 95, and 120 cm by hand tapping 6.35-cm-diameter, 15.24-cm-long cylindrical brass samplers horizontally into the pit walls then hand excavating soil around the samplers to aid their removal.

Material property testing

Grain-size distribution and porosity tests were performed on soil samples in our laboratory in accordance with ASTM standards (American Society for Testing and Materials 2002). Porosity tests utilized results of specific gravity tests performed on parts of the samples.

Saturated hydraulic conductivity of landslide debris was measured in situ at 10 locations near the monitoring site using a Guelph permeameter (five locations) and an amoozemeter manufactured by Ksat, Inc. (5 locations). Measurements were made at depths of 23-89 cm.

Monitoring

We installed 345 kPa, non-vented, vibrating-wire piezometers manufactured by Slope Indicator, Inc. (+/- 0.345 kPa accuracy) into the borehole at depths of 4.9 m, 7.3 m, and 9.1 m (Figure 3) to monitor pore-water pressures. We also installed one length of coaxial cable that extends the full depth of the borehole to detect shear displacement. The coaxial cable was placed inside 2.5-cm-diameter polyvinyl chloride (PVC) pipe, which was subsequently filled with cement grout to provide rigidity. The borehole was backfilled so that each piezometer was surrounded by sand and was isolated from groundwater conditions at neighboring piezometers by at least 0.9 m of bentonite. The borehole was backfilled with cement grout from a depth of 1 m to the ground surface.

Soil Moisture Corp. 100 kPa tensiometers (+/- 0.25 kPa accuracy) were installed at depths of 30, 60, 95, and 120 cm into undisturbed soil that formed one of the walls of the soil pit. An insulated box containing the tensiometer bodies was buried in the pit during backfilling to protect the water-filled tensiometers from freezing winter temperatures.

The length of the coaxial cable installed in the borehole was measured periodically using time-domain reflectometry (Kane and Beck 1994, 1996). The piezometers and tensiometers were connected to a Campbell Scientific CR10x datalogger that was already in operation at the site. Power to operate the datalogger and instruments was provided by a 12-volt battery that was charged by a voltage-regulated solar panel. Instrument readings were taken hourly and downloaded to a portable computer on a periodic basis. Monitoring data were reduced according to manufacturer specifications following retrieval from the datalogger. Piezometer data were corrected for elevation and temperature. Other monitoring equipment in operation at the site was described in detail by Coe *et al.* (2003). The cable displacement transducer (+/- 0.46 cm accuracy) that provided landslide displacement data used during our study was located 4 m downslope from the borehole, while the soil temperature, rainfall, snow depth, and air temperature sensors were located 8 m downslope from our soil pit.

RESULTS

Soil properties

Soils encountered in the soil pit and borehole were generally classified as silty gravel with sand. Soil color was typically dark yellowish orange or moderate yellowish brown with yellowish gray and greenish gray mottling, and consistency was generally moderately dense to very dense. No apparent shear surfaces or zones were identified during either subsurface exploration. Porosity of the four undisturbed soil samples obtained from the soil pit ranged from 0.39 to 0.54; the average porosity was 0.47. In situ hydraulic conductivity test results ranged from 1.34×10^{-6} m/s – 5.71×10^{-5} m/s; the average hydraulic conductivity was 2.31×10^{-5} m/s. These conductivity values are typical for silty sand to well-sorted sand (Fetter 1994, p. 99). Soil moisture content ranged from moist to saturated; wetter conditions were present below depths of

4.8 m in the borehole and 95 cm in the pit. The apparent water table was encountered at a depth of about a meter in the pit (the pit was backfilled before the water level stabilized).

Landslide displacement and weather

Episodic monitoring of the coaxial cable detected no sign of shear displacement, which indicated that the landslide is deeper than our borehole (9.3 m). Continuous displacement monitoring indicated that the landslide moved throughout the period of record (August 12, 2004-June 4, 2006; beginning date follows post-drilling recovery of water levels at the piezometers), with total displacement of 7.6 m at the monitoring site (Figures 4, 5). Landslide velocity at the monitoring site ranged between 0.7-1.7 cm/d with an average velocity of 1.0 cm/d. Therefore, the average daily displacement was about twice the maximum error of the cable displacement transducer (+/- 0.46 cm accuracy). Displacement data were considered in a relative sense so this level of accuracy was assumed to be inconsequential. Landslide velocity data shown on Figures 4-6 were smoothed by taking the weekly average of the daily average velocity calculated at each measurement time (hourly) with the daily and weekly time intervals centered on the measurement time. Landslide velocity was greatest following snowmelt during spring 2005 (Figure 6) and spring 2006 and relatively constant at other times. Relatively heavy rainfall events generally resulted in short periods of increased landslide velocity.

Shallow pore-water pressures and weather

Tensiometer monitoring indicated that the groundwater table was within about a meter of the ground surface at the soil pit location throughout the monitoring period (Figure 4). Many pore-water pressure increases measured by the tensiometers correlate temporally with rainfall and snowmelt events (Figures 4, 5), but the sequence of sensor response generally differs for these types of events. For example, 2.8 cm of rain fell on September 29, 2005 and pore-water pressure increased within a day at all tensiometers beginning with the shallowest sensor and progressing downward. Similarly, 2.0 cm of rain fell on October 27-28, 2004 and pore-water pressure increased nearly instantaneously at the 30 cm tensiometer and then at successively deeper tensiometers during the next two days. In contrast, snowmelt events tended to temporally correlate with simultaneous pore-water pressure increase at all sensors (e.g., beginning April 2, 2006) or measured first at greatest depth then at progressively shallower depths (e.g., April 1-6, 2005).

Deep pore-water pressures and weather

The three piezometers measured very similar pore-water pressure fluctuations throughout the monitoring period, although pore-water pressures dropped and the vertical component of groundwater flow changed during this time (Figures 4, 5). The total head in the deep (3160.77 m elevation) and middle (3162.60 m elevation) piezometers dropped 2 m during the period of record while the water table dropped below the shallow (3165.04 m elevation) piezometer on April 4, 2005. The head drop occurred at a generally consistent rate during fall and winter seasons, although head increased about 20 cm rather abruptly during late October-early November of both years. Pore-water pressure gradually increased, stabilized, then dropped during spring and early summer 2005, and appears to have been increasing during spring 2006. Total head was greatest at the middle piezometer throughout the monitoring period, indicating that the landslide debris is heterogeneous. The vertical hydraulic gradient was upward toward the shallow piezometer from both middle and deep zones, but was downward from the middle to deep piezometer during the period of record (Figure 5). This downward gradient increased until about October 2005 then generally stabilized.

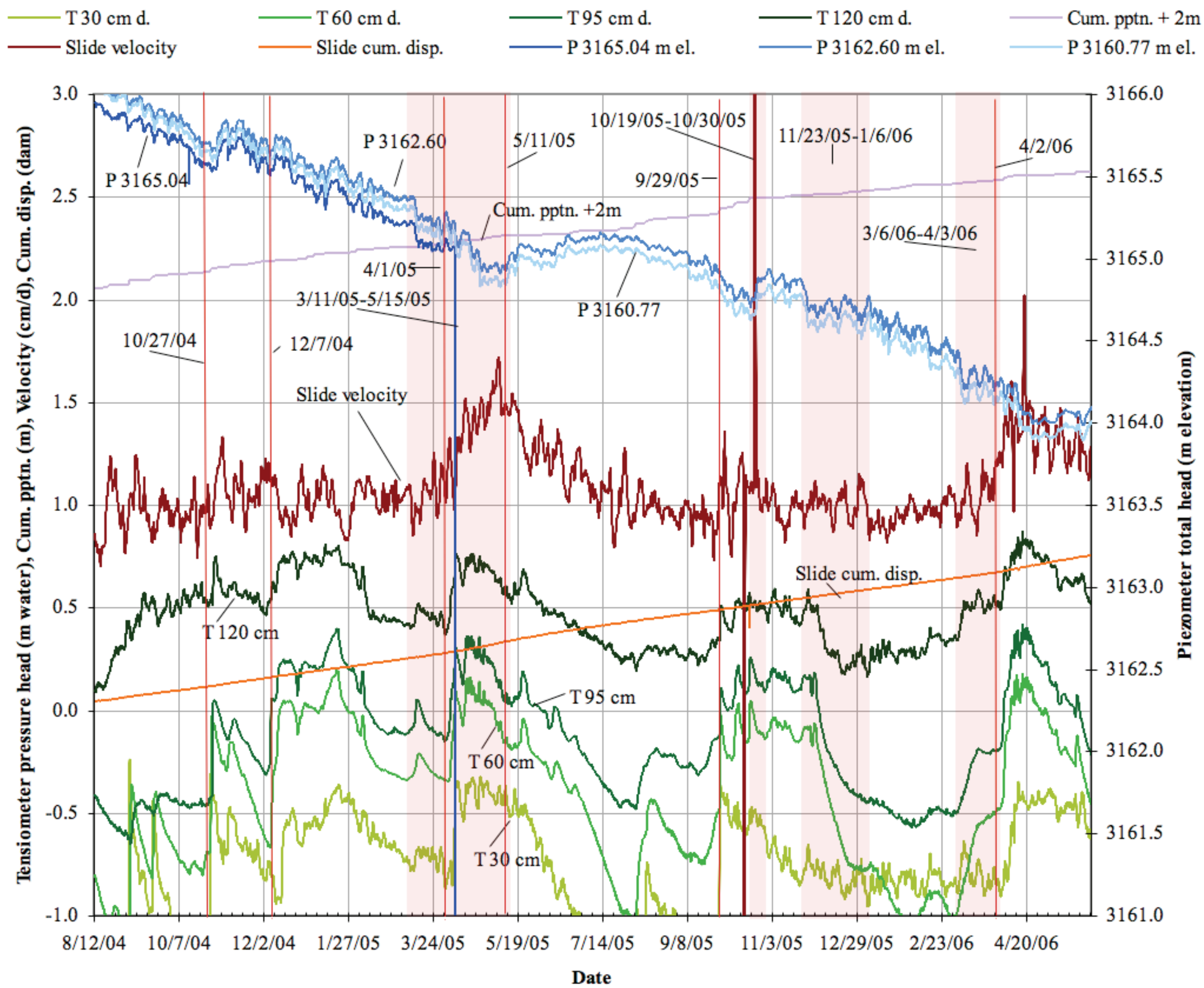

Figure 4. Results of climate, groundwater, and displacement monitoring. Tensiometer data are represented by "T" and sensor depth (d.), and piezometer data are represented by "P" and sensor elevation (el.). Negative tensiometer values indicate soil suction due to unsaturated conditions, while positive values indicate saturated conditions. "Cum. pptn. +2m" represents cumulative precipitation beginning July 3, 2004 with a constant value of 2 m added to improve figure clarity. "Slide cum. disp." represents landslide cumulative displacement. The 3165.04 m elevation piezometer became dry on April 11, 2005 as the groundwater level dropped; hence, no data exist after this date for this piezometer. Dates mentioned in the text are indicated.

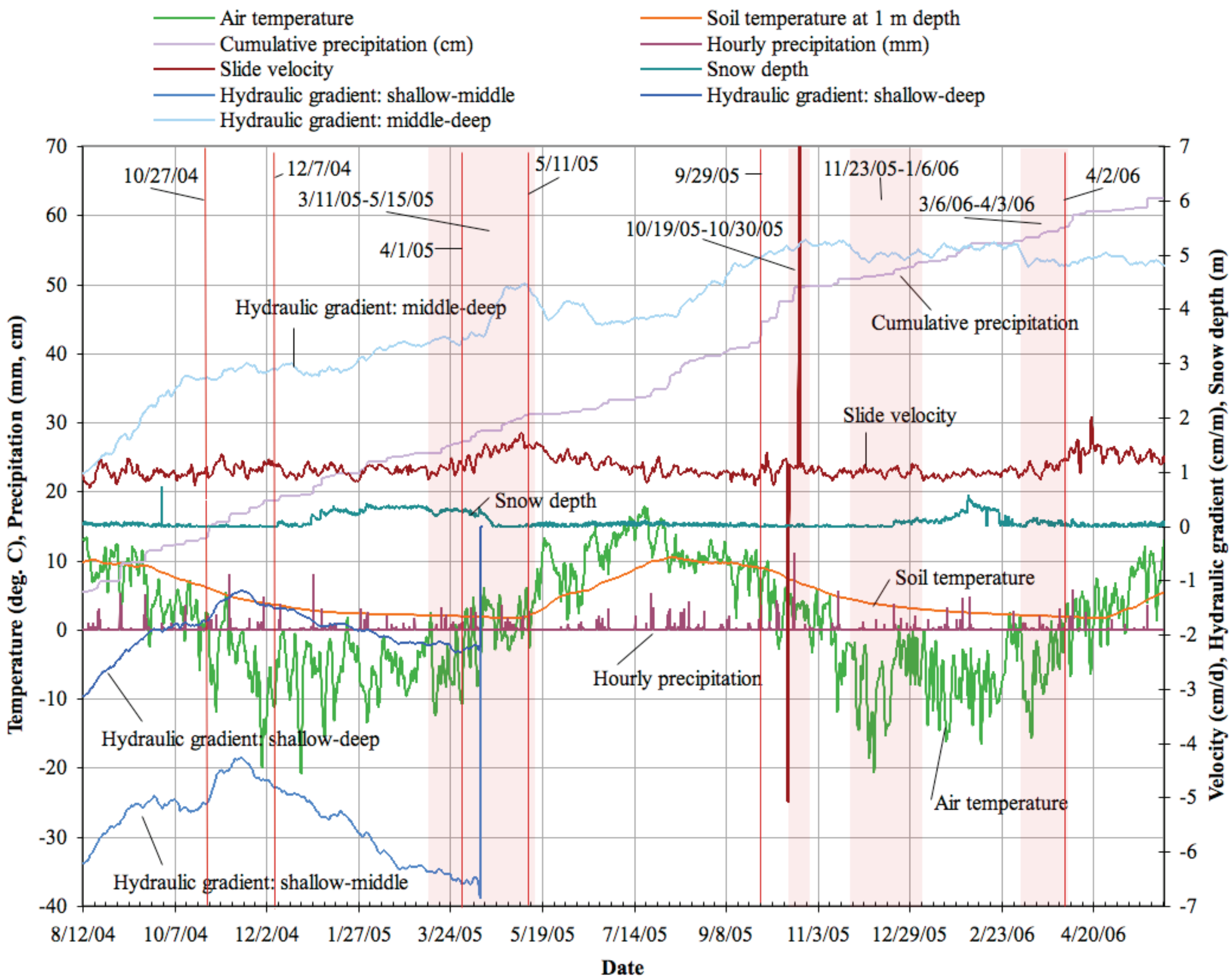

Figure 5. Results of climate, groundwater, and displacement monitoring. Cumulative precipitation was measured beginning July 3, 2004. Hydraulic gradient data are shown between given piezometers with negative values indicating upward groundwater flow and positive values indicating downward groundwater flow. “Shallow” represents the 3165.04 m elevation piezometer, “middle” represents the 3162.60 m elevation piezometer, and “deep” represents the 3160.77 m elevation piezometer. The 3165.04 m elevation piezometer became dry on April 11, 2005 as the groundwater level dropped, hence no “shallow-middle” and “shallow-deep” data exist after this date. Dates mentioned in the text are indicated.

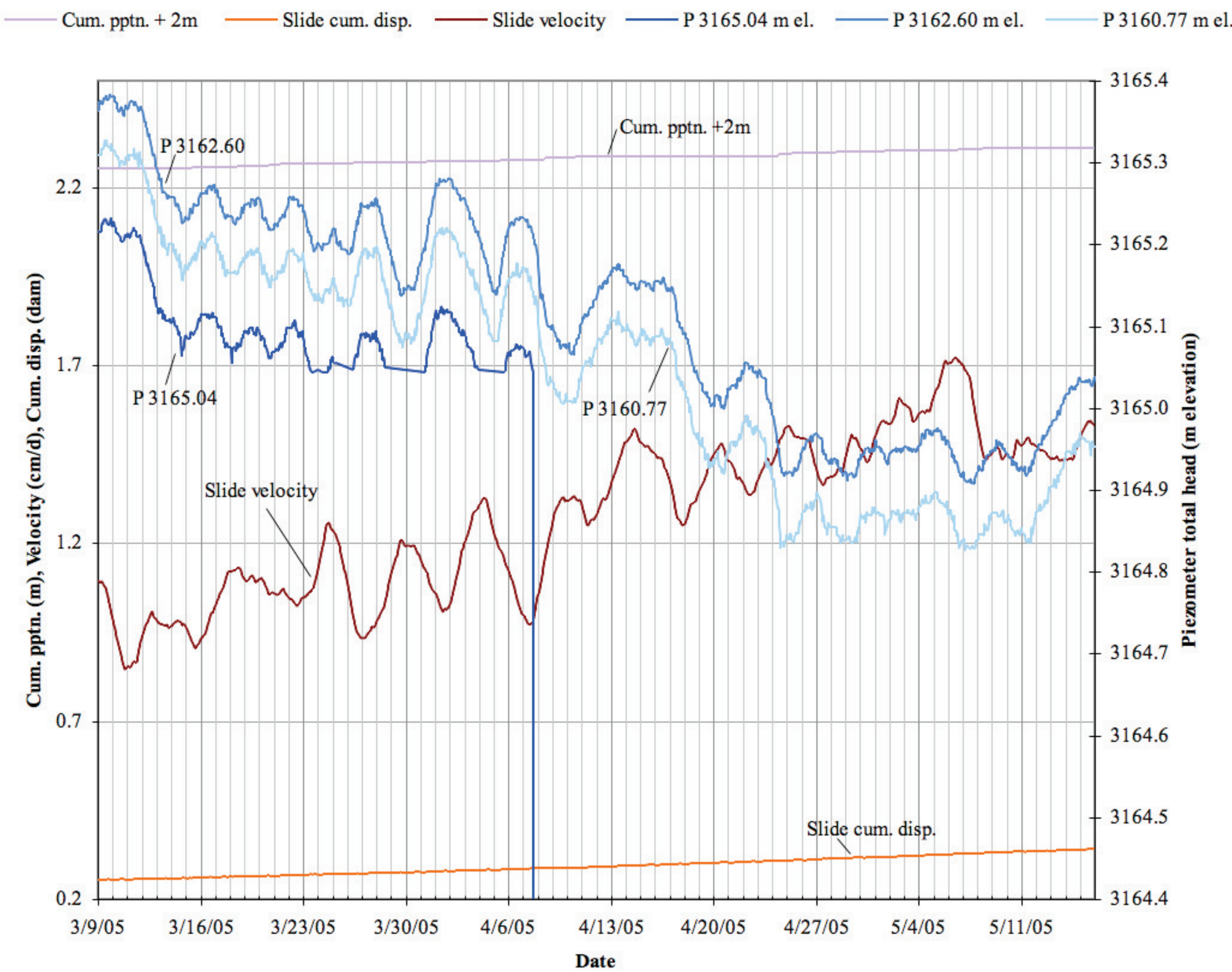

Figure 6. Results of climate, groundwater, and displacement monitoring. Piezometer data are represented by "P" and sensor elevation (el.). "Cum. pptn. +2m" represents cumulative precipitation beginning July 3, 2004 with a constant value of 2 m added to improve figure clarity. "Slide cum. disp." represents landslide cumulative displacement. The 3165.04 m elevation piezometer became dry on April 11, 2005 as the groundwater level dropped; hence, no data exist after this date for this piezometer.

Deep pore-water pressures generally lacked direct correlation with precipitation and snowmelt events at the monitoring site. One instance of apparent direct correlation was the 2.0 cm rainfall event of October 27-28, 2004, which was followed four days later by simultaneous pore-water pressure increases measured by the piezometers. The gradual pore-water pressure increase measured by the piezometers during spring and early summer 2005 probably resulted from snowmelt that occurred during the spring.

Deep pore-water pressures commonly changed in the absence of snowmelt or rainfall events at the monitoring station. For example, pore-water pressure increased at the piezometers on December 7, 2004 and May 11, 2005 in the absence of these events. Repeated cycles of pore-water pressure decrease, stabilization, and increase occurred during periods of minor rainfall or snowmelt on numerous occasions, including March 11-May 15, 2005, November 23, 2005-January 6, 2006, and March 6-April 3, 2006.

Landslide velocity, pore-water pressures, and weather

Landslide velocity changes had variable temporal correlation with rainfall and snowmelt events and shallow and deep pore-water pressure fluctuations (Figures 4, 5). Although deep pore-water pressures near the margin dropped by two meters during the monitoring period, shallow pore-water pressures and landslide velocity were generally consistent, overall.

The landslide generally accelerated as pore-water pressures detected by the tensiometers increased. The snowmelt events of 2005 and 2006 were followed by simultaneous pore-water pressure increase at the tensiometers and landslide acceleration. Similar conditions were observed following the October 27-28, 2004 rainfall event.

Landslide velocity changes generally did not follow deep pore-water pressure changes detected by the piezometers. For instance, pore-water pressure increases measured by the piezometers during spring-early summer 2005 and October 19-30, 2005, and the overall pore-water pressure decrease of 2 m during the monitoring period were not followed by changes in velocity. On the contrary, deep pore-water pressure changes frequently followed landslide velocity changes. Cycles of landslide acceleration and deceleration accompanied, respectively, by deep pore-water pressure decrease and increase were common during the monitoring period (e.g., Figure 6). Acceleration following 2005 and 2006 snowmelt was followed by abrupt deep pore-water pressure decrease, stabilized pore-water pressure as the landslide reached constant velocity, and pore-water pressure increase as the landslide decelerated. A significant increase-decrease cycle in the downward vertical hydraulic gradient between the middle and deep piezometers also occurred during this period. Three similar cycles of landslide acceleration-deceleration and respective pore-water pressure decrease-increase occurred November 23, 2005-January 6, 2006, although these cycles were of much shorter duration, lasting 13-16 days each (Figure 4). About a dozen cycles occurred March 11-May 15, 2005 (Figure 6) as the landslide generally accelerated following snowmelt.

DISCUSSION

Monitoring at the landslide has provided insight into the characteristics of this landslide and into general relationships between weather, groundwater conditions, and landslide displacement.

Soil characteristics and groundwater conditions

Classification of soils around the monitoring site based on field hydraulic conductivity measurements, visual examination, and laboratory testing provided consistent results; the soil is classified as a silty gravel with sand and has hydraulic properties typical for silty sand. Groundwater pressures within the landslide at our tensiometer site temporally responded to rainfall and snowmelt in general agreement with field and laboratory measurements of soil properties, hence infiltration at the monitoring site appears to occur through soil pores, rather than through fractures or local zones of higher hydraulic conductivity that we did not identify.

The groundwater table is located near the ground surface at the monitoring site, which appears to be characteristic within most of the landslide. Shallow groundwater is suggested by landslide acceleration that occurs contemporaneously with precipitation and snowmelt events, assuming that elevated groundwater pressures accompany these events and trigger landslide acceleration. The common occurrence of ponds, springs, and groundwater seepage zones on the landslide also suggests that groundwater is located near the ground surface.

Regional hydrologic effects on groundwater within the landslide

The regional groundwater system (groundwater around but outside of the landslide) appears to affect groundwater conditions near the landslide margin at our monitoring site. The pore-water pressure response to rainfall and snowmelt events was gradual and relatively sustained at the piezometers compared to at the tensiometers, if it was identifiable at all, as illustrated by pore-water pressure changes that followed spring 2005 snowmelt (Figure 4). In contrast, the pore-water pressure response to rainfall and snowmelt events was abrupt and generally direct at the tensiometers. Some damping of infiltration events in the piezometer record likely occurred due to the greater depth of the piezometers than the tensiometers. This damping of the piezometer record also suggests that groundwater along the margin was affected by other sources, such as lateral groundwater flow from outside of the landslide. In addition, groundwater may have been leaking from the landslide through its margin at the monitoring site, possibly due to decreasing groundwater levels outside of the landslide or due to the landslide displacing past soil outside of the landslide that has relatively higher hydraulic conductivity. This potential leakage is suggested by the decrease in landslide saturated thickness at the piezometers from 71% to 60% of the assumed landslide thickness (14 m) during the monitoring period while the saturated thickness remained at a generally constant 93% at the location of the tensiometers. The apparent isolation of groundwater conditions within the landslide indicated by tensiometer data agrees with the hydrological independence of the landslide proposed by Baum and Reid (2000), but changing groundwater conditions along the landslide margin measured by the piezometers suggests that isolation is not complete. The lack of groundwater level decrease at the tensiometers while it steadily decreased at the piezometers suggests that the conditions resulting in decrease along the landslide margin are recent and dynamic. We expect to see the groundwater table drop at the location of the tensiometers in the near future if the groundwater table continues to drop along the margin, which would reinforce the idea that groundwater is leaking through the landslide margin.

Groundwater effects on landslide displacement

Landslide displacement at the monitoring site appears to have generally been directly affected by groundwater conditions within the landslide, but not by groundwater conditions along the landslide margin. Landslide velocity changes generally positively correlated with pore-water pressure changes detected by the tensiometers but did not correlate with pore-water pressure changes detected by the piezometers. This lack of correlation is illustrated by the generally constant landslide velocity during spring-summer 2005 and October 19-30, 2005 periods of elevated pore-water pressure measured by the piezometers. The lack of correlation is also illustrated by generally constant overall landslide velocity during the monitoring period while pore-water pressure dropped by 2 m at the piezometers. This lack of dependence of landslide velocity on pore-water pressures measured along the landslide margin also suggests that pore-water pressure decrease along the margin is a local condition. Decreased pore-water pressures along the landslide margin should have resulted in increased effective strength of the landslide material being sheared, yet the landslide did not slow. The apparent dependence of landslide velocity on pore-water pressures within the landslide as measured by the tensiometers suggests that long-term ground-water level decrease within the landslide due to drought or other conditions could result in slowing of the landslide or cessation of movement altogether. Similarly, long-term ground-water level increase due to prolonged wet conditions could result in overall landslide acceleration.

Landslide displacement characteristics and effects on groundwater conditions

Soil sheared at the landslide margin and base near our monitoring site was apparently dilative, as suggested by the pore-water pressure response measured at the piezometers during periods of landslide acceleration and deceleration. These periods include snowmelt events of 2005 and 2006, and repeated acceleration-deceleration cycles of March 11- May 15, 2005, November 23, 2005-January 6, 2006, and March 6-April 3, 2006. Dilation of landslide debris within basal and marginal shear zones appears to have occurred at an accelerating rate during landslide acceleration and resulted in decreasing pore-water pressures within and near shearing debris as groundwater flowed into larger soil pores and fractures that opened during dilation. Downward vertical hydraulic gradients occasionally increased during dilation as water was essentially sucked into dilating debris along the base of the landslide, as illustrated by monitoring results of March 24-April 10, 2005. Decreasing pore-water pressures during dilation appear to have caused the shearing landslide debris to strengthen and the landslide to subsequently decelerate. Deceleration may have caused consolidation of previously dilated landslide debris and consequent pore-water pressure increase. Increasing pore-water pressures during this deceleration and consolidation period may have resulted in subsequent, similar cycles of acceleration and deceleration. Experimental studies performed using a constant-stress ring-shear device (Moore and Iverson 2002) and controlled landslides (Iverson *et al.* 2000) have documented behavior very similar to that described here. Iverson (2005) developed a mathematical model to explain this type of behavior. Dilation of landslide debris during displacement can result in debris flow (e.g., Johnson and Rodine 1984; Fleming *et al*. 1989; Gabet and Mudd 2006) if sufficient water is present to maintain relatively high pore-water pressures and prohibit strengthening of dilating landslide debris. There appears to be insufficient groundwater and surface water at the landslide to permit this type of rapid failure, as evidenced by apparent dilatant strengthening during landslide acceleration.

CONCLUSION

We found that active landslide debris near the monitoring site is deeper than 9.3 m. Groundwater conditions were observed to vary considerably with distance from the landslide margin. Subdued, gradual, seasonal pore-water pressure increases in response to spring snowmelt were observed near the margin, and rapid, short-lived pore-water pressure fluctuations in response to precipitation and snowmelt events were observed just 17.9 m away toward the axis of the slide. Groundwater level dropped by about 2 m at the landslide margin during the 22 months of record (August 13, 2004-June 4, 2006), but remained nearly steady, on average, 17.9 m farther into the slide. The landslide moved during the entire monitoring period at our monitoring site with an average velocity of 1.0 cm/d and total displacement of 7.6 m. Velocity was greatest following spring snowmelt and generally positively correlated with increased pore-water pressure measured within the landslide 21.3 m from the landslide margin. Pore-water pressure measured along the landslide margin showed an inverse relation with landslide acceleration, probably due to dilation of landslide debris during accelerated shear. Several cycles of acceleration and deceleration accompanied, respectively, by pore-pressure decrease and increase along the landslide margin were also identified. These cycles appear to have involved landslide acceleration accompanied by dilation of shearing landslide debris and subsequent decreasing pore-water pressures, strengthening of shearing debris and landslide deceleration. Deceleration may have been accompanied by contraction of sheared landslide debris and increasing pore-water pressures, which frequently resulted in a subsequent episode of acceleration.

REFERENCES

AMERICAN SOCIETY FOR TESTING AND MATERIALS 2002. *Annual Book of ASTM Standards, 4.08*. American Society for Testing and Materials, Philadelphia, Pa.

BAUM, R. & REID, M. 2000. Ground water isolation by low-permeability clays in landslide shear zones. *In:* BROMHEAD, E., DIXON, N. & IBSEN, M-L. (eds) *Landslides in Research, Theory and Practice.* Thomas Telford, London, 139-144.

COE, J., ELLIS, W., GODT, J., SAVAGE, W., SAVAGE, J., MICHAEL, J., KIBLER, J., POWERS, P., LIDKE, D. & DEBRAY, S. 2003. Seasonal movement of the Slumgullion landslide determined from Global Positioning System surveys and field instrumentation, July 1998-March 2002. *Engineering Geology*, **68**, 67-101.

CRUDEN, D. & VARNES, D. 1996. Landslide types and processes. *In:* TURNER, A. & SCHUSTER, R. (eds) *Landslides: Investigation and Mitigation.* Transportation Research Board National Research Council, Washington, D.C., 36-75.

DIEHL, S. & SCHUSTER, R. 1996. Preliminary geologic map and alteration mineralogy of the main scarp of the Slumgullion landslide. *In:* VARNES, D. & SAVAGE, W. (eds) *The Slumgullion Earth Flow: A Large-Scale Natural Laboratory*. U.S. Geological Survey Bulletin 2130, 13-19.

FETTER, C. 1994. *Applied Hydrogeology.* Macmillan College Publishing Company, Inc., New York.

FLEMING, R., BAUM, R. & GIARDINO, M. 1999. *Map and Description of the Active Part of the Slumgullion Landslide, Hinsdale County, Colorado*. U.S. Geological Survey Geologic Investigations Series Map I-2672.

FLEMING, R., ELLEN, S. & ALGUS, M. 1989. Transformation of dilative and contractive landslide debris into debris flows – an example from Marin County, California. *Engineering Geology*, **27**, 201-223.

GABET, E. & MUDD, S. 2006. The mobilization of debris flows from shallow landslides. *Geomorphology*, **74**, 207-218.

IVERSON, R. 2005. Regulation of landslide motion by dilatancy and pore pressure feedback, *Journal of Geophysical Research*, **110**, 16 p.

IVERSON, R., REID, M., IVERSON, N., LAHUSEN, R., LOGAN, M., MANN, J. & BRIEN, D. 2000. Acute sensitivity of landslide rates to initial soil porosity. *Science*, **290**, 513-516.

JOHNSON, A. & RODINE, J. 1984. Debris flow. *In:* BRUNSDEN, D. & PRIOR, D. (eds) *Slope Instability*. Wiley, London, 257-361.

KANE, W. & BECK, T. 1994. Development of a time domain reflectometry system to monitor landslide activity. *In: Proceedings of the 45th Highway Geology Symposium*, Portland, Ore., 163-173.

KANE, W. & BECK, T. 1996. Rapid slope monitoring. *Civil Engineering*, **66**(6), 56-58.

LIPMAN, P. 1976. *Geologic Map of the Lake City Caldera Area, Western San Juan Mountains, Southwestern Colorado*. U.S. Geological Survey Miscellaneous Investigation Series Map I-962.

MESSERICH, J. & COE, J. 2003. *Topographic Map of the Active Part of the Slumgullion Landslide on July 31, 2000, Hinsdale County, Colorado.* U.S. Geological Survey Open-File Report 03-144.

MOORE, P. & IVERSON, N. 2002. Slow episodic shear of granular materials regulated by dilatant strengthening. *Geology*, **30**(9), 843-846.

PARISE, M. & GUZZI, R. 1992. *Volume and Shape of the Active and Inactive Parts of the Slumgullion Landslide, Hinsdale County, Colorado*. U.S. Geological Survey Open-File Report 92-216.

SAVAGE, W. & FLEMING, R. 1996. Slumgullion landslide fault creep studies. *In:* VARNES, D. & SAVAGE, W. (eds) *The Slumgullion Earth Flow: A Large-Scale Natural Laboratory*. U.S. Geological Survey Bulletin 2130, 73-76.

SHARP, W., MARTIN, R. & LANE, M. 1983. *Mineral Resource Potential of the Powderhorn Wilderness Study Area and Cannibal Plateau Roadless Area, Gunnison and Hinsdale Counties, Colorado.* U.S. Geological Survey Miscellaneous Field Studies Map MF-1483-A.

VARNES, D. & SAVAGE, W. (eds) 1996. *The Slumgullion Earth Flow: A Large-Scale Natural Laboratory*. U.S. Geological Survey Bulletin 2130.